Indian Journal of Science and Technology, *Vol 11(44), DOI: 10.17485/ijst/2018/v11i44/131757, November 2018*
ISSN (Print) : 0974-6846
ISSN (Online) : 0974-5645

Prediction and Experimental Validation of Peak Temperature in Friction Stir Welded AA2024 with AA5083 by Response Surface Methodology

R. Raja, Sabitha Jannet* and D. Emmanuel Sam Franklin

Department of Mechanical, Karunya Institute of Technology and Sciences, Coimbatore – 641114, Tamil Nadu, India

Abstract

Objective: The work aims at prediction of the peak temperature using Response Surface Methodology. **Methods/ Statistical Analysis:** Dissimilar Aluminum Alloys AA2024 and AA5083 O were friction stir welded. A fifteen run 3 factorial 3 level Box Behnken design was conducted and temperature generated were measured at both sides of the alloys. Thermocouples were employed for the same. The temperature was recorded and studies conducted. Response surface plots were used to obtain the peak temperature and effect of various parameters. **Findings:** The relationship between the process parameters and the temperature were established using ANNOVA. Mathematical models were development which can apply for future predictions. The traverse speed, rotational speed and the tool profile contributed to the temperature generation. The peak temperature was obtained at 1200 rpm, 25 m/min and threaded cylindrical tool pin profile. **Application/Improvements:** The temperature at the re-treating side was recorded to be higher compared to the advancing side.

Keywords: Anova, Heat Input, Mathematical Modeling. Peak Temperature, RSM

1. Introduction

A solid-state metal joining process Friction stir Welding changed the whole perspective of metal joining in automobile, ship and aircraft industries[1]. FSW of numerous joint changed into put up-weld heat treated and the remaining tensile strength (UTS) turned into 336 MPa[2]. The pulsed method induces an improved stirring primarily based at the alternation of darkish and light bands, whose chemical composition is near AA 2050 and AA 7449 respectively. An assumption of incompressible fluid flow obtained by a rotating disk was considered to build a three-dimensional model to calculate material flow during friction stir welding[3,4]. The tensile strength of the different joints was found to be increasing with a decrease in heat input[5].

Increasing the rotating speed, results in the transmission of the higher field of temperature distribution from the region of low melting point material to other. The more upper-temperature distribution field is found in the contact area between the shoulder and specimen[6]. The thermoelectric effect between dissimilar materials was used to detect temperature variations, due to geometrical variations of the work piece or due to parameter changes[7]. The reduction within the preheating time can result in the decrease in the stirring effect of the welding zone and shorter preheating time results in weld defects[8]. The impact of the tool rotation on the temperature distribution has been studied for FS welded AA2024-T3 plates[9]. Thermal stresses contribute to a significant part of stresses in the whole process[10–12].

The temperature distribution was found to be unique since there was no uniform load under the tool and the higher temperature was noted on the advancing side compared to the

retreating side[13,14]. The ratio of tool rotation speed to welding speed affected the heat input proportionally[15].

**Author for correspondence*

2. Materials and Methods

In this study, sheets of dissimilar AA 5083-O and AA 2024 alloys with a thickness of 6 mm was used for welding. Various alloying elements for the selected AA alloy and 6 mm pin diameter. Experiments were performed according to full factorial design and parameter details used for experimentation are given in Table 1. To measure the temperature profile, two K-type thermocouples of 1.5 mm diameter were located on both side of the weld at a depth of approximately 1 mm from the surface. Thermocouples were placed at 10 mm distance from the weld center line. The measured peak temperature at different process parameters are given in Table 2.

The significance of the model is assured by the value of F which is 39.25. In this case B, C, A^2, B^2, C^2 are significant model terms. Values greater than 0.1000 indicate the model terms are not significant.

The value of F being 48.35 indicates the significance of the model. In this case B, C, A^2, B^2, C^2 are significant model terms. Values greater than 0.1000 indicate the model terms are not significant as shown in Tables 3, 4.

$$\mathrm{SQRT(TEMP\ 2024)} = 17.7257 + 0.222054 * A + 0.356747 * B + 0.326956 * C + -0.189107 * AB + 0.0306324 * AC + -0.0752058 * BC + -3.34701 * A^2 + -1.43784 * B^2 + 0.142968 * C^2 \quad (1)$$

Table 1. Various alloying elements for the selected AA alloy

Element	Cr	Cu	Fe	Mg	Mn	Si	Ti	Zn	Al
AA 5083-O	0.05	0.10	0.40	4.90	0.40	0.40	0.15	0.25	Bal
AA2024 T4	.1	4.9	.5	1.8	.9	.5	.15	.25	Bal.

Table 2. ANOVA test results for temperature at AA 5083 side

Analysis of variance table [Partial sum of squares – Type III]						
Source	**Sum of Squares**	**df**	**Mean Square**	**F Value**	**p-value**	**Prob > F**
Model	49.85	9	5.54	39.23	0.0004	significant
A-TOOL PROFILE	0.39	1	0.39	2.79	0.1555	
B-TRAVESRING SPEED	1.02	1	1.02	7.21	0.0436	
C-ROTATIONAL SPEED	0.86	1	0.86	6.06	0.0572	
AB	0.14	1	0.14	1.01	0.3604	
AC	3.753E-003	1	3.753E-003	0.027	0.8769	
BC	0.023	1	0.023	0.16	0.7055	
A^2	41.36	1	41.36	292.9	< 0.0001	
B^2	7.63	1	7.63	54.06	0.0007	
C^2	0.075	1	0.075	0.53	0.4975	
Residual	0.71	5	0.14			
Lack of Fit	0.31	3	0.10	0.51	0.7159	not significant
Pure Error	0.40	2	0.20			
Cor Total	50.56	14				

Table 3. ANOVA test results for temperature at AA2024 side

Analysis of variance table [Partial sum of squares - Type III]						
Source	**Sum of Squares**	**df**	**Mean Square**	**F Value**	**p-value**	**Prob > F**
Model	49.06	9	5.45	48.35	0.0002	significant
A-TOOL PROFILE	0.53	1	0.53	4.69	0.0826	
B-TRAVESRING SPEED	0.96	1	0.96	8.52	0.0331	
C-ROTATIONAL SPEED	0.83	1	0.83	7.34	0.0423	
AB	0.18	1	0.18	1.63	0.2575	
AC	2.570E-003	1	2.570E-003	0.023	0.8859	
BC	2.932E-003	1	2.932E-003	0.026	0.8782	
A^2	39.19	1	39.19	347.65	< 0.0001	
B^2	6.89	1	6.89	61.15	0.0005	
C^2	1.02	1	102	9.03	0.0299	
Residual	0.56	5	0.11			
Lack of Fit	0.40	3	0.13	1.62	0.4033	not significant
Pure Error	0.16	2	0.082			
Cor Total	49.62	14				

Table 4. The coefficient of determination values

R-Squared	0.9886	0.9860
Adj R-Squared	0.9682	0.9609
Pred R-Squared	0.8637	0.8856
Adeq Precision	19.852	18.097

$$\mathrm{SQRT\ (TEMP\ 5083)} = 16.6717 + 0.257077 * A + 0.346469 * B + 0.321606 * C + -0.21449 * AB + -0.0253485 * AC + -0.0270723 * BC + -3.25805 * A^2 + -1.3664 * B^2 + 0.525068 * C^2 \quad (2)$$

The above Equations 1 and 2 states the relationship and percentage effect of various parameters on the temperature generated during the welding process.

Response Surface Methodology (RSM) is an appropriate tool for the conduction of experiments.

The Figures 1 and 2 shows the response plots obtained for the temperature with respect to various process parameters. It is an adequate mechanism to develop mathematical models for physical processes. It also analyses the premiere combination of entering parameters and explicit the values of the parameters in the shape of surface graphs and contour plots. To recognize the influencing parameters on the temperature distribution, the mathematical model was developed. Response surface plots and contour plots which are the symptoms of possible independence of these factors on the responses has been advanced. These reaction contours can assist inside the prediction of the responses for any location of the experimental domain. The most temperature has been taken from the peak of the response plot. Contour plots display a particular round mound shape indicative of possible independence of factors with the response. Technology of contour plot can be greater complicated for 2nd-order responses as compared to the simple series of parallel strains that may arise with first-order models. Once the motionless factor is discovered, it is also required to characterize the reaction floor inside the immediate vicinity of the point. Characterization is the technique of identifying whether or not the immobile point is a minimal response or maximum response or a saddle factor.

To categorize this, it is required to study it via a contour plot. The reaction surfaces of tensile behavior from

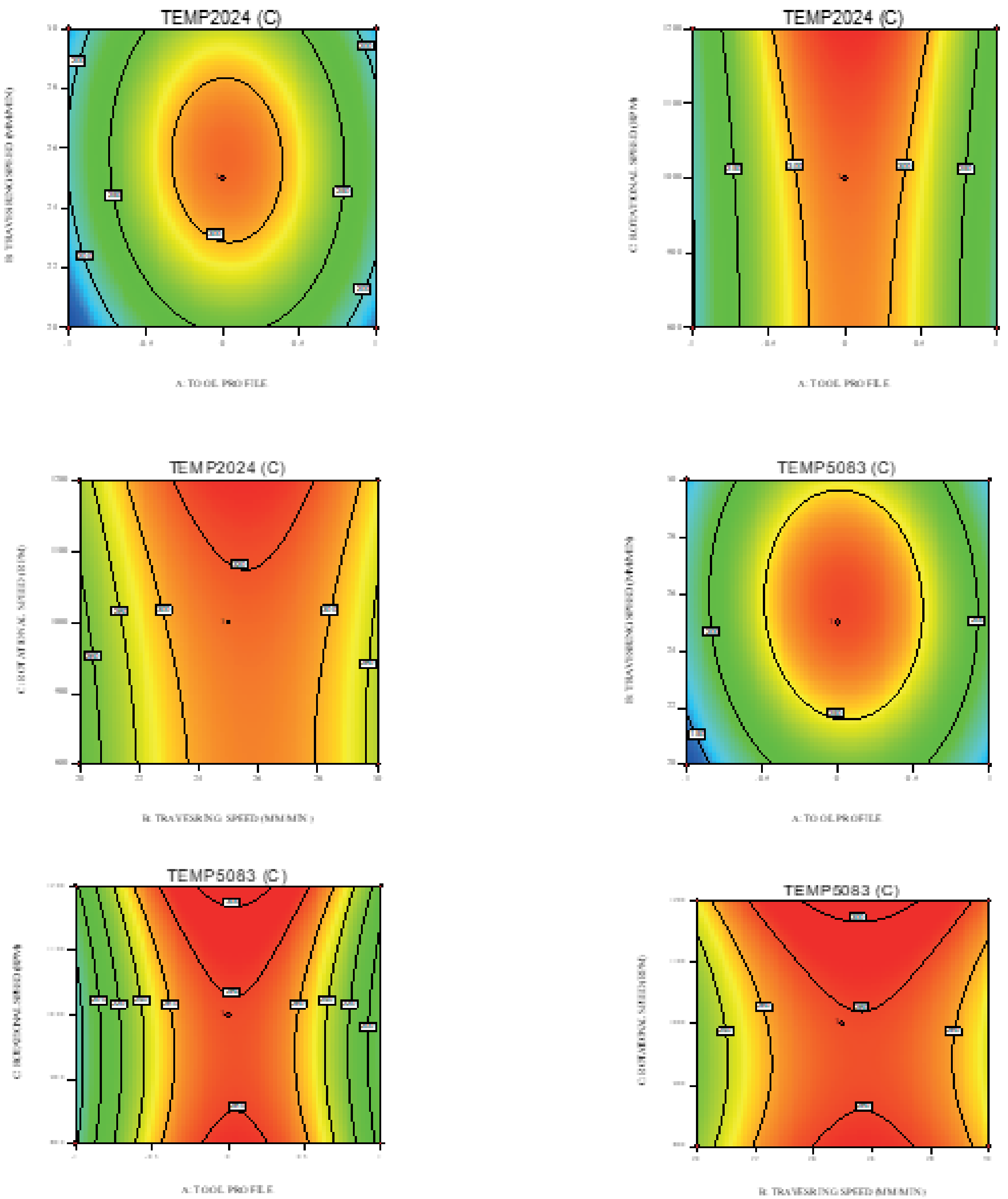

Figure 1. Countour plot for the various process parameters with temperature as response.

the graphs were analyzed. The response surfaces of temperature from the charts have been investigated. The corresponding FSW parameters for maximum UTS, wear resistance and minimum wear rate are Threaded cylindrical pin profile, rotational tool speed of 1200 rpm, welding speed of 25 mm/min.

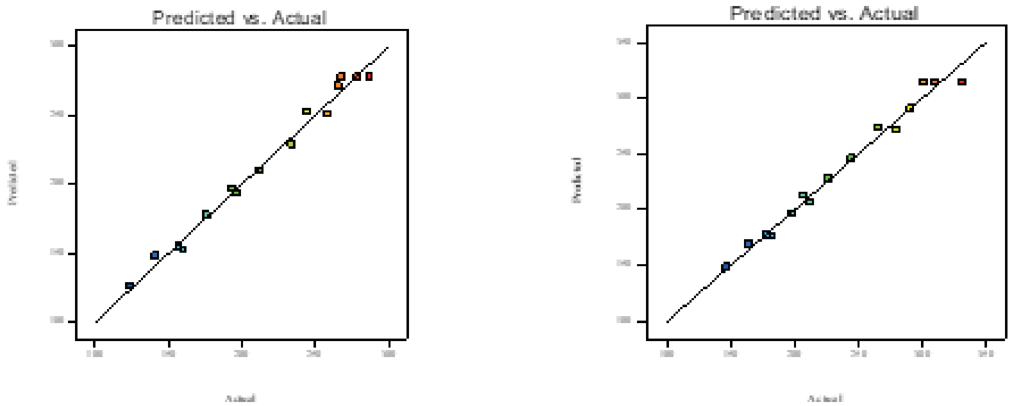

Figure 2. Predicted vs. actual values for the temperature on both the sides of the joint.

3. Results and Discussions

3.1 Effect of Traversing Speed

The temperature at the joint increased with decrease in traverse speed as shown in Figure 3. This may be because of the way that at lesser traverse speed introduces dwell time of the tool with work piece leading to preheating of the joint and after that the heat created because of friction may assume an essential part in heat generation.

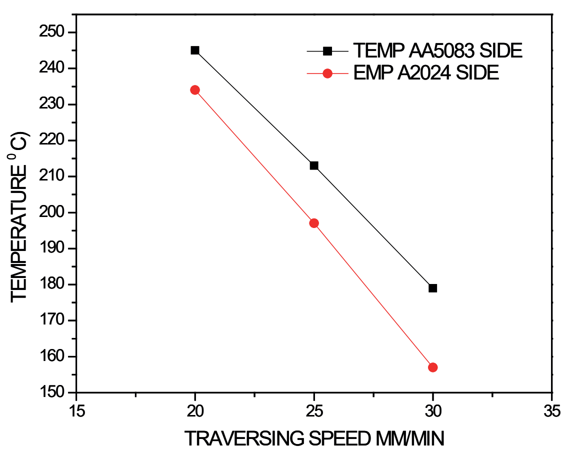

Figure 3. Effect of traversing speed on temperature.

3.2 Effect of Tool Rotational Speed

From the Figures 4 and 5 we can infer that the heat generated increases with increase in tool rotational speed. The cause for this trend may be attributed to the frictional heat which is generated as a result of the tool rotational speed and increase in speed leads to more friction and heat.

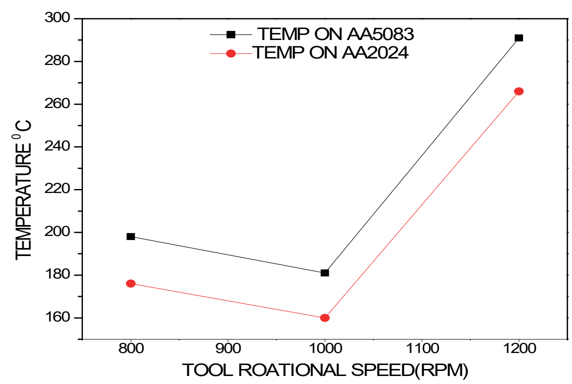

Figure 4. Effect of tool rotational speed on temperature.

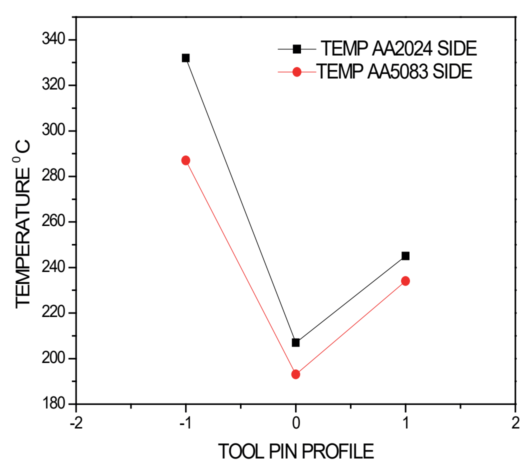

Figure 5. Effect of tool pin profile on temperature.

3.3 Effect of Tool Pin Profile

The various tool profiles used for this study were pentagon, threaded and square pin profiles.

3.4 Microstructure Analysis

Various tool profiles have produced different grain structure for Heat Affected Zone and Thermo mechanically affected zones, these are depicted in the Figure 6 respectively. Lesser heat generation and grain growth have been observed. In contrast to this trend, reduction in cooling rate during minimum traversing speed causes reduction in the residual stresses.

Due to this phenomenon, the degree of embrittlement along with low heat input also results in a small degree of recovery and re-crystallization. This enhances the density of defect leading to the increment in strength level. The interaction time seems to be adequate enough for mitigating the discontinuities. This factor could be attributed for the absence of voids.

Exhibits the grain structure fabricated at rpm while having the same traversing speed with the tool profile of threaded cylinder. This results in the increase of heat input and reduction of cooling rate. It also results in the decrease in defect concentration and the increase in residual stress. Eventually it causes a higher volume fraction of voids.

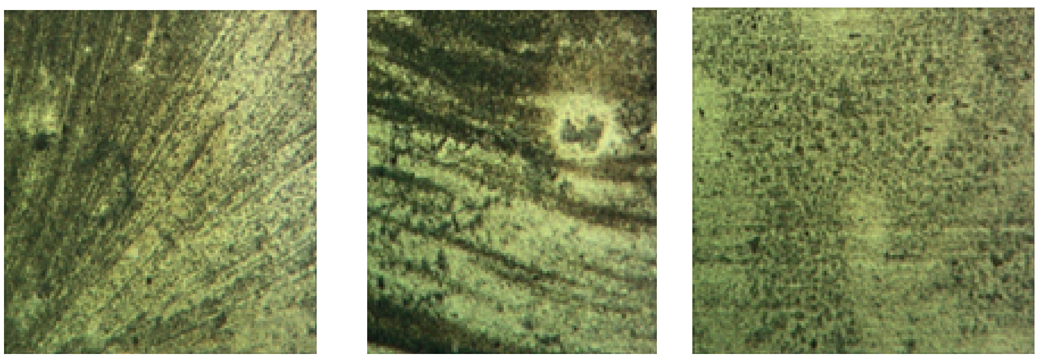

Figure 6. Optical micrograph of HAZ 1) Pentagon pin profile, 2) Square pin profile, 3) threaded pin profile.

4. Conclusion

The results showed that the heat generation during FSP strongly depends on rotational and transverse speed and the temperature was not tested in the welding zone. The temperature displayed on the monitoring unit for AA-2024 was less than AA-5083. For the same tool profile and with increasing RPM the temperature difference was in between 15-20 degrees. The peak temperature at the retreating side is higher compared to the advancing front. The temperature increases with an increase in tool rotational speed and decreases with increase in traversing speed. From the statistical analysis, it was observed that the peak temperature on both sides is strongly influenced by the rotational speed (P = 82.65% for AS and P = 85.65% for RS) than the welding speed.

5. References

1. Jagathesh K, Jenarthanan MP, Babu PD, Chanakyan C. Analysis of factors influencing tensile strength in dissimilar welds of AA2024 and AA6061 produced by friction stir welding. Journal of Australian Journal of Mechanical Engineering. 2017; 15(1):19–26. https://doi.org/10.1080/14484846.2015.1093229
2. Eberl I, Hantrais C, Ehrtsrom JC, Nardin C. Friction stir welding dissimilar alloys for tailoring properties of aerospace parts. Journal of Science and Technology of Welding and Joining. 2010; 15(8):699–705. https://doi.org/10.1179/136217110X12813393169499
3. DebRoy T, Bhadeshia HKDH. Friction stirs welding of dissimilar alloys – a perspective. Journal of Science and Technology of Welding and Joining. 2010; 15(4):266–70. https://doi.org/10.1179/174329310X12726496072400

4. Tavares SMO, Castro RAS, Richter-Trummer V, Vilaca P, Moreira PMGP, de Castro PMST. Friction stirs welding of T-joints with dissimilar aluminum alloys: Mechanical joint characterization. Journal of Science and Technology of Welding and Joining. 2010; 15:312–8. https://doi.org/10.1179/136217109X12562846839114
5. Guo JF, Chen HC, Sun CN, Bi G, Sun Z, Wei J. Friction stir welding of dissimilar materials between AA6061 and AA7075 Al alloys effects of process parameters. Materials and Design (1980-2015). 2014; 56:185–92.
6. Hussein SK. Analysis of the temperature distribution in friction stir welding of AA 2024-T3 and AA 6061-T6 using finite element method. U.P.B Science Bulletin. 2016; 78(4):119–32.
7. De Backer J, Bolmsjo G. Thermoelectric method for temperature measurement in friction stirs welding. 2013; 18:558–65.
8. Zhang Z, Zhang HW. Numerical studies of preheating time effect on temperature and material behaviours in friction stir welding process. Journal of Science and Technology of Welding and Joining. 2007; 12:436–48. https://doi.org/10.1179/174329307X214386
9. Tutum CC, Deb K, Hattel JH. Multi-criteria optimization in friction stir welding using a thermal model with prescribed material flow. Journal of Materials and Manufacturing Processes. 2013; 28:816–22. https://doi.org/10.1080/10426914.2012.736654
10. Soundararajan V, Zekovic S, Kovacevic R. Thermo-mechanical model with adaptive boundary conditions for friction stirs welding of Al 6061. International Journal of Machine Tools and Manufacture. 2005; 45(14):1577–87. https://doi.org/10.1016/j.ijmachtools.2005.02.008
11. Khandkar MZH, Khan JA, Reynolds AP. Prediction of temperature distribution and thermal history during friction stir welding: Input torque based model. Science and Technology of Welding and Joining. 2003; 8:165–74. https://doi.org/10.1179/136217103225010943
12. Verma S, Meenu, Misra JP. Study on temperature distribution during friction stir welding of 6082 aluminum alloy. Materials Today: Proceedings. 2017; 4:1350–6. https://doi.org/10.1016/j.matpr.2017.01.156
13. Bisadi H, Rasaee S, Farahmand M. Experimental study of the temperature distribution and microstructure of plunge stage in friction stir welding process by the tool with triangle pin. Archives of Civil and Mechanical Engineering. 2014; 61(3):483–93. https://doi.org/10.2478/meceng-2014-0028
14. Bindu KDB, Trivedi PAM. Effect of size of tool on peak temperature and viscosity during friction stir welding of AA6061-T6 aluminum alloy using hyper works. International Journal of Innovative Research in Science, Engineering. 2013; 2:914–9.
15. Hao DD, Tra TH, Hoa VC. Study of effect of friction stir welding parameters on impact energy of AA7075-T6. Tạpchi Khoa hocva Congnghe. 2016; 54(1):99–108.